Dynamics of Melting and Recrystallization in a Polymeric Micellar Crystal Subjected to Large Amplitude Oscillatory Shear Flow

Carlos R. López-Barrón,[1,*] Lionel Porcar,[2] Aaron P. R. Eberle,[3] and Norman J. Wagner[4]
[1]ExxonMobil Chemical Company, Baytown, Texas, 77520, USA
[2]Institut Laue-Langevin, BP 156, F-38042 Grenoble Cedex 9, France
[3]National Institute of Standards and Technology, Center for Neutron Research, Gaithersburg, Maryland 20899, USA
[4]Center for Neutron Science, Department of Chemical Engineering, University of Delaware, Newark, Delaware 19716, USA
(Received 22 January 2012; published 21 June 2012)

Shear-induced structural transitions of a micellar cubic phase during large amplitude oscillatory shear flow is studied with time-resolved oscillatory rheological small angle neutron scattering. This technique allows us to resolve the structural changes within a cycle of oscillation. By applying a strain rate near the critical melting shear rate, melting and recrystallization occurs in a cyclic mode. The maximum degree of order is observed when the shear stress reaches a plateau value during the large amplitude oscillatory shear cycle, whereas melting is maximized at the strain rate wave peaks. This structural evolution confirms the cyclic mechanism of sticking and sliding of 2D hexagonal close-packed layers [I. W. Hamley *et al.*, Phys. Rev. E **58**, 7620 (1998)].

DOI: 10.1103/PhysRevLett.108.258301 PACS numbers: 47.57.Qk, 61.05.fg, 64.75.Yz

Formation of two-dimensional hexagonal close-packed (hcp) layers upon applying shear deformation to colloidal crystals has been described theoretically by Loose and Ackerson [1] and observed experimentally via small angle scattering measurements [2–10]. Under steady shear, the layered structure has a lower resistance to flow with respective shear thinning response. At even higher shear rates, the layered structure is destroyed (i.e., the system melts [11]), leading to a Newtonian or shear thickening viscous behavior [1,12].

Oscillatory shear has also been used to direct self-assembly in colloidal systems [7–14]. McMullan and Wagner used rheo-light scattering to study self-assembly and microstructural changes as a function of time of colloidal particles directed by large amplitude oscillatory shear (LAOS) [7]. Torija *et al.* used a flow small angle x-ray scattering cell to study the grain alignment during plastic deformation of a block copolymer micellar cubic phase subjected to LAOS (with low strain amplitude = 50%) [14]. However, to date, there are no reports of the structural changes in colloidal systems within a cycle of oscillation. This is due to a limitation in time resolution, inherent to scattering techniques [in particular small angle neutron scattering (SANS)]. Consequently, only time-average scattering is normally measured [7,12–16]. To our knowledge, only one attempt to describe the structural evolution within a LAOS cycle was made by Shin *et al.* [13]. They reported the small angle x-ray scattering profiles, for a diblock copolymer melt, at each quarter of cycle, which is insufficient to elucidate the dynamics of structure evolution.

In this study, we use time-resolved oscillatory rheo-SANS (tOrSANS) to measure true time-resolved SANS during oscillatory shear. This technique consists of stroboscopically synchronizing the collection of the streaming SANS scattering intensity with the oscillatory shear deformation imposed on the sample. The position of the moving boundary is monitored through an analog I/O channel from the rheometer and synchronization is achieved by an electronic card triggering a *top-off* event at each maximum in the voltage signal. The oscillation period (T) is divided into a number of time bins (n_b) to achieve meaningful statistics. The scattering intensity is collected over a prescribed number of oscillatory cycles (n_c) and superimposed. Here, we used $n_b = 48$ and $n_c \sim 300$. The time resolution is defined by the jitter in the analog signal that triggers the top-off event which is submillisecond. A prerequisite for choosing a material to be interrogated with tOrSANS is that it behaves the same for each subsequent cycle. All tOrSANS measurements were performed on the D22 SANS beam line (ILL, Grenoble, France) using a stress-controlled rheometer (Anton-Paar MCR 501) with a frequency (ω) of 1 rad/s and a titanium Couette cell of 0.5 mm gap [17]. The incident neutron beam was aligned parallel to the velocity gradient direction ($\nabla\vec{v}$), and the scattering intensity represents the 2D projection of the flow-vorticity ($\vec{v}$-$\vec{e}$) plane.

In this Letter, we report the shear-ordering directed by LAOS of a micellar cubic phase of the triblock copolymer $(EO)_{106}$-$(PO)_{68}$-$(EO)_{106}$ (Pluronic F127), dissolved in the protic ionic liquid, ethylammonium nitrate (EAN). EAN is advantageous over water in that it has negligible vapor pressure; however, it must be dried and is hygroscopic. F127 is an amphiphilic copolymer that forms spherical micelles in water and in EAN [5,18,19]. Jiang *et al.* reported the layered structure of a 20 wt% F127 aqueous solution induced by steady shear [5], which they related to the shear thinning behavior observed in a wide range of

shear rates. The same aqueous solution was subjected to LAOS by Hyun *et al.* [18]. They reported a square-shaped stress response that indicates a strong strain thinning within the LAOS cycle, which was rationalized by sticking and sliding of the layers [3,18].

tOrSANS measurements are performed on a 24 wt% solution of F127 in EAN. Below 22 °C, the solution forms a disordered structure and behaves as a Newtonian low-viscosity liquid, whereas above 22 °C it becomes a self-sustaining gel with a body-centered cubic (bcc) lattice structure [19]. The sample was loaded at 15 °C, and subsequently heated to 40 °C. By applying a shear rate $\dot{\gamma} > 10\ s^{-1}$, the system forms a hcp layered structure, and it melts completely at $\dot{\gamma} > 200\ s^{-1}$ [19]. LAOS measurements were performed using a strain-controlled rheometer (ARES-G2, TA Instruments) with concentric cylinders geometry and with $\omega = 1$ rad/s, allowing 10 delay cycles were before collecting 4 sampling cycles, which were then averaged. The same number of delay cycles was used in the tOrSANS measurements. The dynamic strain sweep (Fig. 1) shows that the linear viscoelastic regime is restricted to very low strain values ($\gamma_0 < 0.2\%$), above of which a weak strain overshoot (increase of G'') is observed followed by a shear thinning behavior, spanning at least four decades of strain. The same LAOS behavior was observed by Hyun *et al.* [18] for a F127 20 wt% aqueous solution in the "hard gel" region. They associate the increase in G'' to an increase in the dissipation energy due to microstructural break-up, and the shear thinning to aligning and sliding of layers in the flow direction. The plateau value of $G' > 10^4$ Pa is consistent with a "hard gel" cubic structure [20,21].

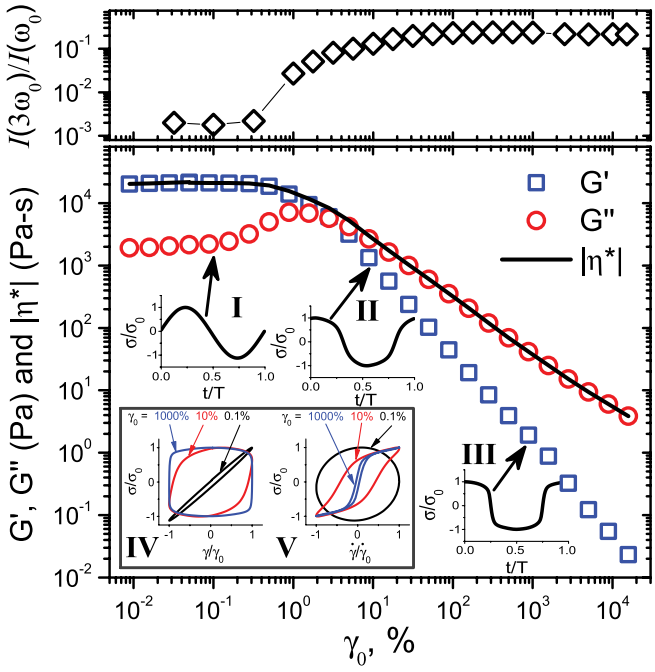

FIG. 1 (color online). Dynamic moduli and complex viscosity vs strain amplitude of 24 wt% F127/EAN solution at 40 °C. Insets I, II, and III give the stress response at $\gamma_0 = 0.1\%$, 10%, and 1000%, respectively. Insets IV and V show the normalized elastic and viscous Lissajous curves, respectively, for the same strain amplitudes. Top: Ratio of the third to the first harmonic as a function of γ_0.

The nonlinearity of the stress response is quantified by the ratio of the third to the first harmonics, $I(3\omega)/I(\omega)$ [22]. As expected, this ratio is negligible in the linear regime (see Fig. 1), and grows at $\gamma_0 > 0.2\%$ (at the onset of the strain overshoot) before it reaches an asymptotic value at $\gamma_0 > 100\%$, where the system displays shear thinning behavior. Similar behavior was reported by Daniel *et al.* in a diblock copolymer cubic phase [21]. The insets I, II, and III in Fig. 1 show the normalized stress (wave form) response at three selected strain amplitudes. The corresponding elastic and viscous Lissajous curves are given in insets IV and V, respectively. In the linear regime, the stress wave form is sinusoidal and the Lissajous curves are ellipsoidal, whereas in the nonlinear regime, the stress wave form and the elastic Lissajous curve become rectangular; i.e., the stress quickly reaches a maximum when the strain peaks and then plateaus until the strain peaks again. The same behavior was observed for the F127 aqueous solution [18].

Hamley *et al.* [3] proposed a "stick-slip" flow mechanism to explain the rectangular Lissajous patterns. The layers stick due to the short-range interaction potential between micelles at the start of the sharp increase of the stress signal, which corresponds to zero strain rate, $\dot{\gamma}_0 = 0$ [see Fig. 2(a)]. The slip (layers sliding one over the other) occurs at the peak of the strain rate and corresponds to the destruction of the stacking sequence. Recent efforts to give mechanical interpretation of LAOS response for ordered micellar structures can be found in the literature [22]. However, these interpretations based on the mechanical response alone can only speculate on the underlying microstructural transitions. This lack of simultaneous measurement of microstructure and rheological properties is addressed here.

This study focuses on the nonlinear viscoelastic regime, near the melting region, i.e., by applying strain rates ($\dot{\gamma}_0 = \gamma_0\omega$) near the critical shear rate for melting ($\approx 200\ s^{-1}$ [19]). Fig. 2(a) displays the LAOS data at $\gamma_0 = 10\,000\%$ (i.e., $\dot{\gamma} = 100\ s^{-1}$) in the form of a 3D Lissajous curve, whose 2D projections onto the planes stress vs. strain and stress vs. strain rate are the elastic and viscous Lissajous curves. The LAOS data are normalized with the amplitude of the corresponding wave forms (γ_0, $\dot{\gamma}_0$, and σ_0). The normalized stress wave forms and the Lissajous curves are nearly identical for the strain amplitudes studied here ($1000\% \leq \gamma_0 \leq 15\,000\%$) [23], corresponding to a constant value of $I(3\omega)/I(\omega)$ (Fig. 1).

SANS patterns in the $\vec{v}$-$\vec{e}$ plane during LAOS at $\gamma_0 = 10\,000\%$ are shown in Figs. 2(b) and 2(c) and at

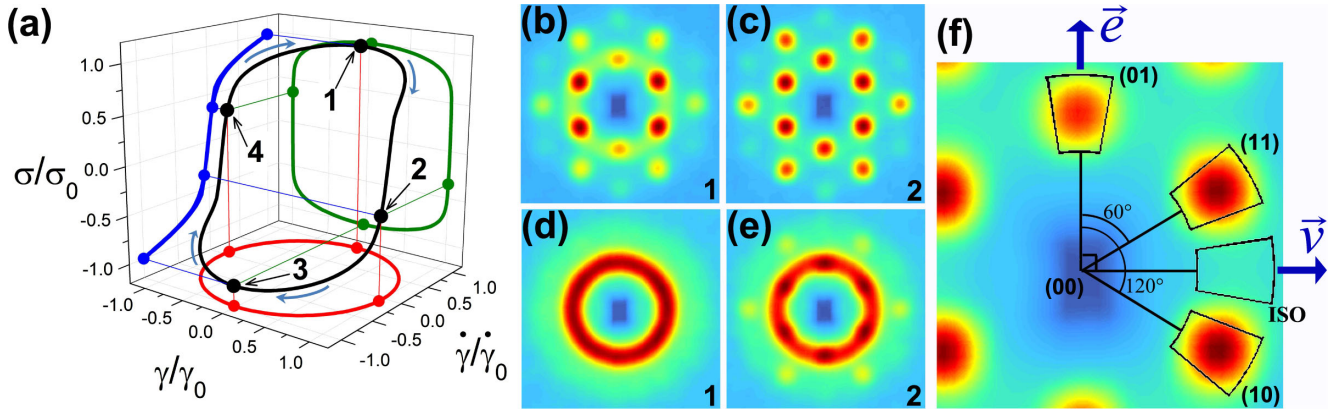

FIG. 2 (color online). Stress response and SANS profiles during LAOS. (a) Normalized Lissajous curve showing the stress response as a function of strain and shear rate during LAOS with $\gamma_0 = 10\,000\%$. (b) and (c) are the SANS patterns in the flow ($\vec{v}$)-vorticity ($\vec{e}$) plane corresponding to points 1 and 2, respectively, in the Lissajous plots for $\gamma_0 = 10\,000\%$. The corresponding SANS patterns for $\gamma_0 = 15\,000\%$ are shown in (d) and (e), respectively. (f) Shows a detail of (c) with the indexing of the first diffraction ring for a hcp-layered structure according to Loose and Ackerson [1]. The indicated annular sections are the areas used to calculate intensities: I_{01}, I_{10}, I_{11}, and I_{ISO}, which are used to calculate DOO and DOS [Eqs. (1) and (2)].

$\gamma_0 = 15\,000\%$ in Figs. 2(d) and 2(e). The SANS pattern in Fig. 2(c) exhibits the typical diffraction spots of hcp layers [1] with sixfold symmetry of the first three diffraction orders. SANS patterns in Figs. 2(b) and 2(d) correspond to the stress maximum [point 1 in Fig. 2(a)], where $\gamma(t) = 0$ and $\dot{\gamma}(t)$ is maximum. Whereas Figs. 2(c) and 2(e) correspond to zero shear rate [point 2 in Fig. 2(a)]. Clearly, the onset of the stress plateau corresponds to a state of higher ordering, as shown by the sharper diffraction spots. The isotropic halo observed in the first ring in Figs. 2(b) and 2(e) indicates partial meting of the hcp layers. Melting results in shear thinning within the LAOS cycle [points 1 and 3 in Fig. 2(a)]. Fig. 2(d) displays complete isotropy of the diffraction pattern. By subtracting the intensity of the isotropic halo, I_{ISO}, from that of the diffraction spots, I_{11}, we define the degree of order

$$\mathrm{DOO} = \frac{I_{11} - I_{\mathrm{ISO}}}{I_{11}}, \qquad (1)$$

where I_{ISO} and I_{11} are computed by integrating the scattering intensity in the equal-area annular sections indicated in Fig. 2(f). Fig. 3(b) shows that degree of order (DOO) evolves cyclically with twice the frequency of the mechanical excitation [shown in Fig. 3(a)]and in general decreases with the strain amplitude. Within a cycle, maximum DOO is observed after reaching maximum strain amplitude (when the shear rate and stress are reversing direction and sign, respectively). Minimum DOO occurs slightly after the maximum shear rate amplitude is reached.

Notice that the intensity of the (01) peak, I_{01}, is always lower than that of the (11) peak, I_{11}, whereas (11) and (10) peaks have the same intensity (see Fig. 2). Loose and Ackerson explained this lack of symmetry due to the sliding of adjacent layers [1]. Sliding can occur in two ways, by motion of neighboring layers in a zig-zag path or in a parallel straight line path. The latter results in a complete suppression of the (01) spot while only partial intensity reduction would result from the zig-zag motion [1]. Therefore, we can quantify the degree of sliding (DOS)

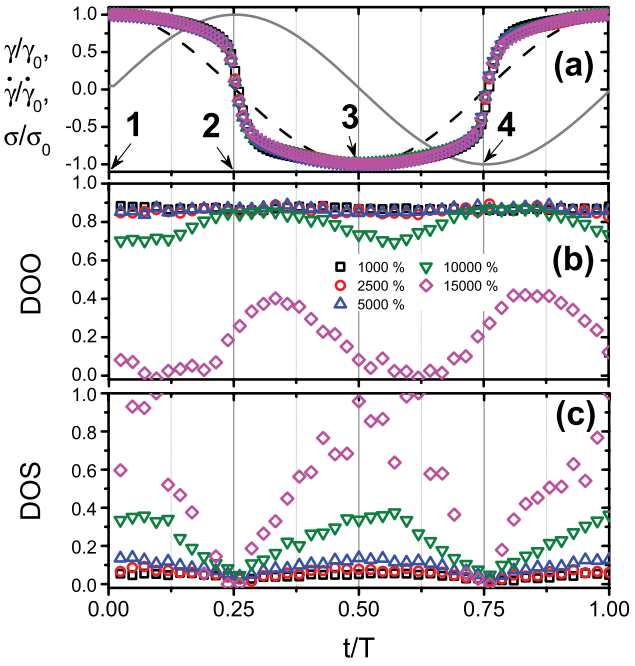

FIG. 3 (color online). (a) Normalized mechanical variables (solid line: γ/γ_0, dashed line: $\dot{\gamma}/\dot{\gamma}_0$ and symbols: σ/σ_0), (b) degree of order, and (c) degree of sliding as a function of normalized time during a LAOS cycle with strain amplitudes indicated by symbols. The numbers in (a) correspond to the same points indicated in the Lissajous curve [Fig. 2(a)].

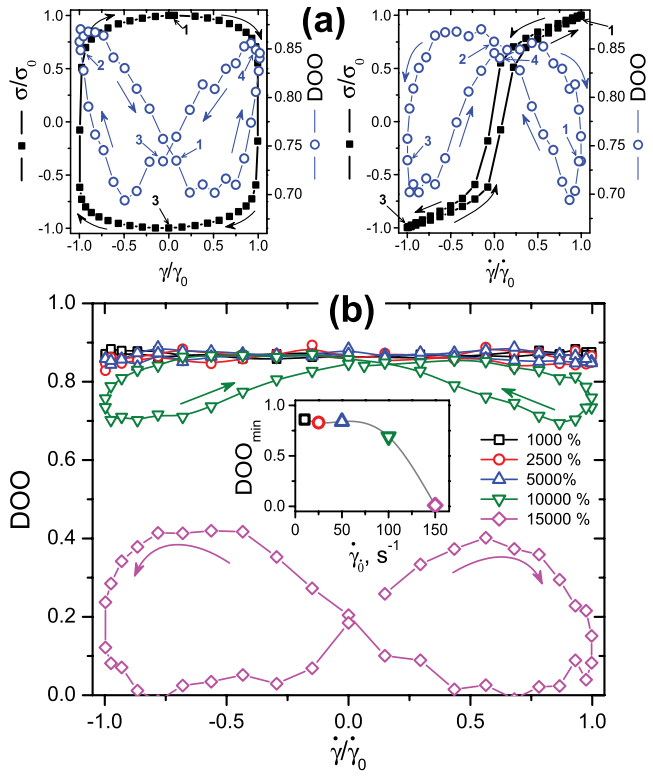

FIG. 4 (color online). (a) σ/σ_0 and DDO vs γ/γ_0 and $\dot{\gamma}/\dot{\gamma}_0$ during a LAOS cycle at $\gamma_0 = 10\,000\%$. The numbers indicate the same points in Figs 2(a) and 3(a). (b) DOO vs $\dot{\gamma}/\dot{\gamma}_0$ for the indicated values of γ_0. Inset: Minimum DOO in the LAOS cycles as a function of $\dot{\gamma}_0$. The arrows in all the plots indicate the positive time progression in the LAOS cycles.

by the ratio between intensities of the (01) and (11) spots [see Fig. 2(f)]

$$\mathrm{DOS} = 1 - \frac{I_{01} - I_{\mathrm{ISO}}}{I_{11} - I_{\mathrm{ISO}}}. \quad (2)$$

Fig. 3(c) shows the cyclic evolution of DOS during a single LAOS cycles. Clearly, the maximum sliding occurs slightly after the peak of the shear rate, i.e., when layer sliding occurs. On the other hand, minimum sliding, i.e., maximum layer sticking, occurs when the stress is zero. Overall, the cyclic evolution of DOO and DOS are consistent with the "stick-slip" flow mechanism [3], as the "sticky" state has the maximum order, whereas the "sliding" state (where DOS is maximum) coincides with the minimum ordering.

A structural analog to the Lissajous curves is constructed by plotting DOO vs γ_0 and $\dot{\gamma}_0$. These curves plotted along with the "mechanical" Lissajous curves give a more clear picture of the interrelation between microstructural evolution and mechanical response during LAOS. These are shown in Fig. 4(a) for $\gamma_0 = 10000$. The start-up of the LAOS cycle is indicated with the number 1, and it progresses towards points 2, 3, and 4 in the same sequence indicated in Figs. 2(a) and 3(a). The butterfly shapes of the curves in Fig. 4(a) indicate that melting and recrystallization occurs at different rates during the LAOS cycle. Melting is a strong function of the increasing strain rate and stress, whereas recrystallization progresses more gradually as $\dot{\gamma}(t)$ decreases. Contrarily, recrystallization shows a stronger dependence on strain than melting. These observations suggest that the dynamics of melting and recrystallization during LAOS is a convoluted function of the state of stress and the amount and rate of deformation. Consequently, a rational interpretation of the LAOS stress response requires direct measurements of the time-dependent microstructure, as shown here.

The butterfly shapes of the plots shown in Fig. 4(a) are observed at $\gamma_0 \geq 2500\%$ [Fig. 4(b)], i.e., at $\dot{\gamma}_0 \geq 25\ \mathrm{s}^{-1}$. This is the same shear rate range where partial melting is observed in steady flow [19]. Finally, the minimum DOO value in the LAOS cycles ($\mathrm{DOO}_{\mathrm{min}}$) is plotted vs. $\dot{\gamma}_0$ in the inset of Fig. 4(b). $\mathrm{DOO}_{\mathrm{min}}$, which is a measure of the level of melting, shows a constant value at $\dot{\gamma}_0 < 100\ \mathrm{s}^{-1}$ and decreases at $\dot{\gamma}_0 \geq 100\ \mathrm{s}^{-1}$. This is in accordance to the behavior observed under steady flow [19].

In summary, we found that melting and recrystallization of the F127/EAN hcp layered structure occurs cyclically (with twice the strain frequency) during a single LAOS cycle. We confirmed that the structural evolution probed with tOrSANS is in agreement with the "stick-slip" flow mechanism proposed by Hamley *et al.* [3]; i.e., the micelle layers stick to each other (and hence DOO is maximum and DOS is minimum) when the shear rate is low, whereas, they slip (where DOO is minimum and DOS maximum) when the shear rate reaches a peak value. tOrSANS is a powerful method to study the dynamics of structural changes and the structural origins of the nonlinearities inherent to LAOS measurements of soft materials.

The Institut Laue Langevin (Grenoble, France) is acknowledged for the beam time allocated on D22.

*carlos.r.lopez-barron@exxonmobil.com

[1] W. Loose and B. J. Ackerson, J. Chem. Phys. **101**, 7211 (1994).
[2] J.-F. Berret, F. Molino, G. Porte, O. Diat, and P. Lindner, J. Phys.: Condens. Matter **8**, 9513 (1996).
[3] I. W. Hamley, J. A. Pople, C. Booth, L. Derici, M. Imperor-Clerc, and P. Davidson, Phys. Rev. E **58**, 7620 (1998).
[4] I. W. Hamley, J. Phys.: Condens. Matter **13**, R643 (2001).
[5] J. Jiang, C. Burger, C. Li, J. Li, M. Y. Lin, R. H. Colby, M. H. Rafailovich, and J. C. Sokolov, Macromolecules **40**, 4016 (2007).
[6] G. A. McConnell, M. Y. Lin, and A. P. Gast, Macromolecules **28**, 6754 (1995).
[7] J. M. McMullan and N. J. Wagner, J. Rheol. **53**, 575 (2009).
[8] F. R. Molino, J. F. Berret, G. Porte, O. Diat, and P. Lindner, Eur. Phys. J. B **3**, 59 (1998).

[9] T. M. Slawecki, C. J. Glinka, and B. Hammouda, Phys. Rev. E **58**, R4084 (1998).
[10] K. Mortensen, E. Theunissen, R. Kleppinger, K. Almdal, and H. Reynaers, Macromolecules **35**, 7773 (2002).
[11] B. J. Ackerson and N. A. Clark, Phys. Rev. Lett. **46**, 123 (1981).
[12] M. J. Solomon and J. Vermant, J. Phys.: Condens. Matter **17**, R187 (2005).
[13] G. Shin, N. Sakamoto, K. Saijo, S. Suehiro, T. Hashimoto, K. Ito, and Y. Amemiya, Macromolecules **33**, 9002 (2000).
[14] M. A. Torija, S.-H. Choi, T. P. Lodge, and F. S. Bates, J. Phys. Chem. B **115**, 5840 (2011).
[15] B. J. Ackerson and P. N. Pusey, Phys. Rev. Lett. **61**, 1033 (1988).
[16] P. A. Smith, G. Petekidis, S. U. Egelhaaf, and W. C. K. Poon, Phys. Rev. E **76**, 041402 (2007).
[17] L. Porcar, D. Pozzo, G. Langenbucher, J. Moyer, and P. D. Butler, Rev. Sci. Instrum. **82**, 083902 (2011).
[18] K. Hyun, J. Nam, M. Wilhellm, K. Ahn, and S. Lee, Rheol. Acta **45**, 239 (2006).
[19] C. R. López-Barrón, L. Porcar, and N. J. Wagner (to be published).
[20] S. Hvidt, E. B. Joergensen, W. Brown, and K. Schillen, J. Phys. Chem. **98**, 12320 (1994).
[21] C. Daniel, I. W. Hamley, M. Wilhelm, and W. Mingvanish, Rheol. Acta **40**, 39 (2001).
[22] K. Hyun, M. Wilhelm, C. O. Klein, K. S. Cho, J. G. Nam, K. H. Ahn, S. J. Lee, R. H. Ewoldt, and G. H. McKinley, Prog. Polym. Sci. **36**, 1697 (2011).
[23] See Supplemental Material at http://link.aps.org/supplemental/10.1103/PhysRevLett.108.258301 for raw LAOS data in the form of wave forms and Lissajous curves as well as a movie showing the evolution of SANS patterns in sync with the mechanical excitation and the stress response.